www.rericjournal.ait.ac.th

A Case Study on Corrective Measures of Secondary Control Assisted Microgrids

Sameer Bhambri*, [1], Vivek Shrivastava[#], and Manoj Kumawat

Abstract – *Flexibility and efficiency are the qualities of microgrids which are associated with power delivery and intended to create a system which can adapt to changes in distributed generation output and load demand in an effective and timely way, without sacrificing stability or performance. In order to maintain the power quality requirements, microgrid control solutions should be reliable enough to operate both independently and in conjunction with the utility power network. The paper proposes secondary layer control function in the control hierarchy of microgrid and mechanism behind its implementation to correct frequency and voltage deviations resulted through primary control. Two network forming inverters, feeding a common load are considered for this study. A discretized SVM (space vector modulation) technique is utilized owing to advantages such as high utilization of DC link voltage and low output voltage total harmonic distortion, to convert the modulating signals into pulses for driving the power electronics-based converter/inverter. Computer simulations (Reactive/active power sharing, frequency, voltage, current and voltage tracking versus time) are performed on MATLAB-Simulink software to evaluate the efficacy of the proposed approach.*

Keywords – Control, droop, microgrid, model, secondary

1. INTRODUCTION

The electric power production, its transmission, and distribution have undergone through several development stages, and new techniques are still being developed today. These developments have goals of sustainable future and reliable power supply to the end users. At the start of the 20th century, society began to consolidate formerly dispersed power-producing competitors-typically situated near their end users-into expansive, state-approved monopolies in order to enhance stability and service reliability and guarantee the development of standardised infrastructure for a technology that, within a century of its inception, became a fundamental human necessity [1,2].

The central controls serving as dispatchers for these interconnected generating units led to the development of electrical power engineering, which deploys and optimises computing resources to produce dependable, safe, and efficient electrical power systems. The trend in use of distributed generation systems paved the way for the development of a localised generation-transmission-distribution electrical power system that includes loads, batteries, and distributed generators (DGs). As a single, controllable unit, these units have advantages not just in an environmental pollution terms but also for greater local reliability and risk mitigation because they require less expensive infrastructure [3]. A number of literatures are available with significant efforts put in this direction.

Research published in [4] examines how the secondary control layer in an islanded microgrid is impacted by the intrinsic characteristics/methods of digital communication technology. The simulated results highlight the advantages and disadvantages of each strategy and point out risks that, if adequately avoided or managed beforehand, can avert failures that might otherwise happen.

Authors in [5] proposed their research with an aim of analyzing grid connected inverters in distributed generations. The stability and efficacy of LCL-filter-based current regulated system are challenged by the wide range of grid impedance. This paper shows that the application of active damping contributes to system stabilisation with regard to a wide variety of resonance types. In [6], a four-node real-world laboratory setup that can simulate both distributed generation network scenarios (grid connected as well as islanded) is described. The hardware and software configuration are thoroughly described, with particular attention paid to the dual-core DSP used for control, which is close to industry standards and capable of simulating actual complexity. A thorough experimental part demonstrates the system's primary characteristics.

In the study conducted in [7], advanced control methods for microgrids are reviewed. Control of grid-connected and islanded microgrids using decentralised, distributed, and hierarchical methods is discussed in this study.

The voltage source converter/inverter (VSC/I) plays a significant role and acts as an interface between distributed energy resource and load. This also interfaces load through a filter. The filter's shunt capacitor and dampening resistor values were adjusted to minimise noise and boost power o/p during load current disruptions. The filter capacitor's low impedance acts as

*Electrical Engineering, National Institute of Technology, Plot No FA7, Zone 1, GT karnal Road, Delhi, 110036, India.

[#]Electrical Engineering, National Institute of Technology, Uttarakhand, Srinagar, Pauri (Gharwal)-246174, India.

[1] Corresponding author;
Tel: 8318680612.
E-mail: sameerbhambri@nitdelhi.ac.in

a bypass for harmonics by reversing the converter's harmonic currents, preventing them from entering the load and ensuring voltage support at the node.

A comprehensive collection of examples and digital computer time-domain simulation studies are presented in [3,8] to illustrate the control design processes and desired performance.

The addition of automation, intelligence, and communication like qualities to power electronic based VSCs allows the system to communicate with the utility grid in bidirectional way, resulting in the emergence of the smart grid concept. The voltage and frequency stability, black start operation, reactive and active power regulation, active power filtering capabilities, and energy storage management are all those aspects that are likely to be a part of these smart grids. In [9], focus is laid on new automation techniques in practical microgrid control. New advancements in microgrid control, like the "internet of electricity" or "energy internet," are highlighted. A framework for the internet of electricity that can be used to regulate microgrids is suggested.

In the direction of standardization of microgrids, [10] presents hierarchical control, with its different levels, derived from electrical dispatching standards and ISA-95 in order to incorporate flexibility and smartness into microgrids. Stable connection/disconnection of microgrid to the main utility grid is also a challenge in its operation. In case of a grid failure, [11] outlines a way for implementing a stable deliberate disconnect/reconnect of local grids from the utility electrical network. The grid-connected power converter that uses this control technique functions as an intelligent connection agent (ICA) and changes its mode of operation based on the connection state.

CDC (Conventional droop control) enables the microsource inverters to decentrally control the local frequency, and voltage of the microgrid and the real and reactive power generation of each inverter in an islanded operation. Microsource converters connected to the microgrid with LCL filters provide a weak grid since they act as islands and have a very small moment of inertia. At the PCC, any non-linear load that draws harmonic currents changes the voltage quality because of the drop between the inductors on the grid side of microsource inverters. Due to the inclusion of resonance phenomena, these harmonics may impact the stability of the microgrid and should be handled well [12-15].

When operating in an islanded mode, the output impedances of multiple inverters connected in parallel play a significant role in sharing both active, and reactive power with the load. Any discrepancies in the inverters' output impedances result in distinct operating conditions at the point of common load, which in turn impacts power sharing with the local load. Reactive power, fundamental current component, and harmonic current sharing all get out of sync as a result. On the other hand, active power sharing is controlled by P-ω droop characteristics and remains unchanged till the microgrid's frequency stays constant. The microgrid's frequency stabilises under steady state conditions and stays intact until local load excursions exceed the rated capacity of the inverter[16-18]. The aforementioned issue might be resolved by controlling the output impedance of an inverter. This problem has been extensively discussed in the literature and resolved by adding *VI* (virtual impedance) to the control loop. The goal of adding virtual impedance is to equalise each inverter's per unit output impedance. While applying it, the output impedance type-which can be resistive, inductive, resistive-inductive, or resistive-capacitive-should be carefully chosen. Multiple inverters' output impedances cannot be normalised since line impedances can also range in value. Additionally, changes in the filter's component over time are also problematic [19-23[.

Virtual damping and inertia have also been incorporated in control model of an individual inverter to alleviate the stability issues in microgrids. Analysis and simultaneous optimization of VSG (virtual synchronous generator) and VI (virtual impedance) parameters have been reported in [24-27] with dq based modelling in detail for two bus microgrid.

Considering the aforementioned literature review, the paper focuses on mechanism of the corrective measures taken by secondary layer in the control hierarchy with the following objectives to be met.

1.1 Objectives

1) To discuss control methods in microgrids and to model the proposed MG structure with secondary control.
2) To evaluate and discuss case study of islanded Microgrid with corrective actions of secondary layer control through computer simulations.

2nd section of the paper discusses about main (primary), secondary and tertiary control layer, followed by the microgrid model under study. The simulation results are discussed in section 4th. The paper is concluded in the section 5th with possible future contribution.

2. PRIMARY AND SECONDARY CONTROL LAYER

The main (primary), secondary and tertiary MG control layers are described in this section using the hierarchical control approach as shown in Figure.1. The base layer has the quickest response and governs the device level, whereas the higher layers have a slower response comparatively and govern the system level [2]. The key features of multilayer control system is to regulate reactive and active power flow to provide stable voltage amplitude and frequency, besides adding reactive power compensation, harmonics current sharing and filtering in order to ensure disturbance rejection and power quality standard in microgrids [4,7,10].

In hierarchical control structure, the droop technique is typically employed to enable the concurrent operation of several voltage source inverters sharing loads and confirming power quality standards. By making control over voltage amplitude and frequency, the

primary layer adds virtual inertia, which replicates the inertial characteristics of traditional power systems and guarantees accurate power distribution among the inverters. The second layer of control corrects frequency and the voltage amplitude variations brought on by the droop equations and mechanism behind this is explained in section 3rd. However, at the PCC, power flow between MG and the utility grid is controlled by the third (tertiary) layer [3-7].

The main (primary) layer of an individual voltage source inverter functions on the basis of local measurement only, however the next (secondary) layer control can also be carried out in a similar way either locally or on communication (distributed or centralized) basis between the VSCs. The third (tertiary) control layer, however, needs to be managed centrally via communication channels [3].

The droop control based primary layer is employed to regulate voltage, frequency to further manage the power produced by each VSC (voltage source converter). In the traditional power system, the high power technology that gave rise to the droop control idea allows synchronous alternators (with high inertias) to share the load parallelly by lowering their frequency (*f)* as *P* (real power) on grid rises.

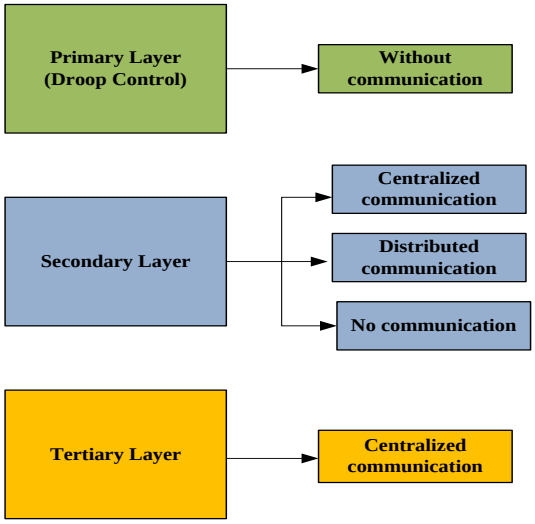

Fig. 1. Hierarchical control layers of microgrid.

Generating units which are coupled electronically to voltage source converters do not possesses inertia features to stabilise the system during synchronisation stages, in contrast to typical traditional power systems. Rather, by providing a very quick response, it offers complete control over the dynamics of the system and transient. Therefore, the droop method electronically emulates the inertial behavior of alternators in the n/w forming converters, controlling the ω (frequency) and *V* (voltage amplitude) proportionate to the *P* (real power) and *Q* (reactive power) components, in order to improvise the stability of MG and coordination of VSCs operating parallelly [2,7].The fundamental droop equations of first (primary) layer of control are given by (1) and (2).

$$\omega_k = \omega_{NOM} - m_{kd} P_k \quad (1)$$

$$V_k = V_{NOM} - n_{kd} Q_k \quad (2)$$

Where[3],

ω_k - angular frequency (in rad/s) of the k^{th} inverter.

P_k - Corresponding active power (in W).

ω_{NOM}- nominal frequency of the system.

m_{kd}- active power-frequency $(\omega_k\text{-}P_k)$ droop coefficient (in rad/Ws).

V_{NOM} - The amplitude of nominal voltage.

n_{kd} - coefficient associated with voltage- reactive power $(V_k\text{-}Q_k)$ droop equation (in V/VAr).

V_k - the k^{th} inverter output voltage (in Volts).

Q_k- reactive power (in Var) associated with k^{th} inverter.

A constant and equal droop coefficient m_{kd} for all inverters results in an equal and accurate active power (P_k) sharing because the frequency of system acts as a global variable that is generated equally between the n/w forming converters in the steady state. The voltage component, on the contrary, is a local variable; hence, even with comparable droop coefficients, there is not ideal reactive (Q_k) power sharing because of the unequal voltage amplitude at various microgrid nodes. This is illustrated by (3) and (4) for two (k = 1,2) network forming inverters[3].

$$m_1 P_1 = m_2 P_2 \quad (3)$$

$$n_1 Q_1 = n_2 Q_2 + V_2 - V_1 \quad (4)$$

As describe in (5), the sinusoidal reference voltage (V_{REF}) of each converter is produced using ω_k, and V_k from the droop control model.

$$V_{REF} = V_k \sin(\omega_k t) \quad (5)$$

The angular frequency/power $(\omega_k\text{-}P_k)$ droop equation incorporates a feed forward term with regard to the real power (P_k) in order to enhance the transient response in V_{REF} (reference voltage), as shown in (6) [3,23].

$$\omega_k = \omega_{nom} - m_k P_k - m_{kdp} \frac{dP_k}{dt} \quad (6)$$

With respect to changes in real power, the gain m_{kdp} supports in having quicker transient response, and the feed-forward signal is related to the derivative $(\frac{dP_k}{dt})$ component. An analogue of the proportional-derivative (PD) control is this droop-compensation term [3]. By relocating closed loop modes, the new term can enhance damping performance.

2.1 VI Loop

In order to ensure harmonic current sharing under the conditions of unbalanced , non-linear loads, lessen the

effect of circulating current and attenuate distortion, the droop approach simulates an impedance at the VSC o/p using an extra closed loop control, which is known as Z_v, (virtual impedance). As stated in (7), the output current determines the inclusion of the *VI* as a new variable in the V_{REF} signal [3,7].

$$V_{REF} = V_k sin(ph) - R_{vk} i_o - L_{vk} \frac{di_{ok}}{dt} \quad (7)$$

Where $ph = \int \omega_k$, L_{vk} and R_{vk} are inductive and resistive components of *VI*, i_{ok} is the k^{th} converter output current.

$$Z_{vk} = R_{vk} + jL_{vk} \quad (8)$$

2.2 Secondary Control

By reducing the frequency & voltage amplitude variations due to the droop based approach, the secondary layer control maintains the power sharing that the first layer had accomplished and returns the values to preset ranges in the steady-state. This layer restores the V_k and ω_k within their predefined ranges by an addition of a corrective term, therefore shifting the droop characteristics up to each unit's original characteristics. The function of secondary control has been illustrated in Figure 2.

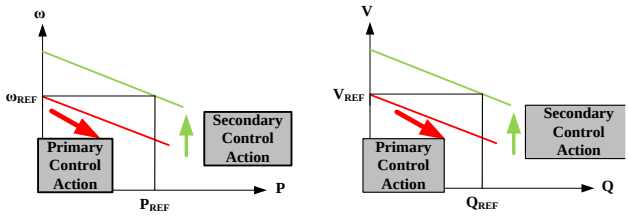

Fig. 2. Secondary and primary actions of microgrid

Notably, with an absence of secondary layer implementation, the impedances and virtual inertia of the droop controlled primary layer cause changes in voltage amplitude and the generation frequency of microgrid , which are reliant on load. Secondary control strategies range from distributed control to central control traffic patterns of communication services [4,7,10]. Table.1 shows a qualitative summary of key features of secondary control technique in terms of their communication scheme, clock drift, communication constraints and bandwidth.

Table.1 Features of secondary Layer

Technique	Communication scheme	Clock drift	Communication constraints	Communication BW
Centralized-control	One to all	No	Robust	High
De-centralized-control	One to all	yes	none	none
De-centralized averaging-control	All to all	No	weak	very high
De-centralized consensus-control	All to all	No	strong	very high

The control block diagram of an individual converter *k*, with inclusion of droop model, virtual impedance model and reference generation scheme has been shown in Figure 3. The power reference values (P_{ref} and Q_{ref}) are considered to be zero in an islanded mode of MG operation.

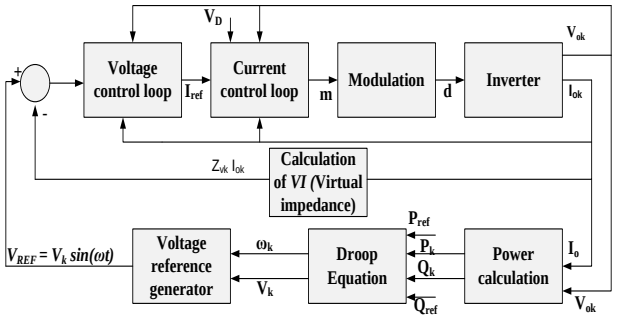

Fig. 3. Droop and virtual o/p impedance control loop.

3. MICROGRID MODEL

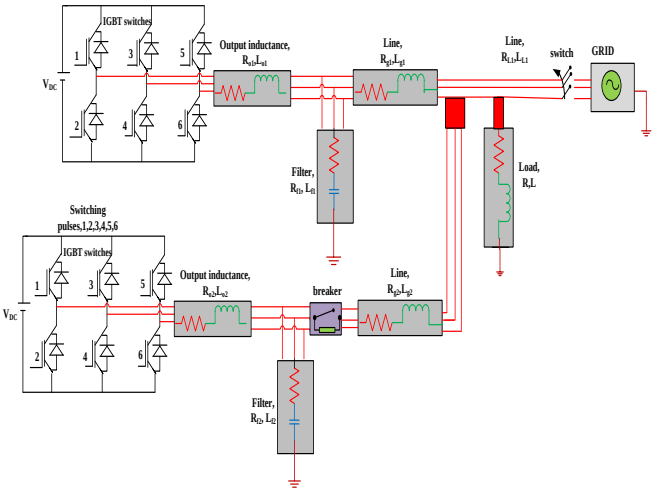

Fig. 4. Two inverter microgrid model.

The detail microgrid model is shown in Figure.4, showing two inverters, their output impedances (R_o,L_o), filter (R_f,L_f), grid (R_g,L_g), line (R_L,L_L) and load (R,L) parameters. V_{DC} is emulated from renewable energy based distributed energy source like solar photovoltaic. Converter consists of six IGBT switches and corresponding pulses are obtained from SVM block. The modelling details are given below.

In order to simplify operation of 3-phase converters and further analysis, the three-dimensional phasor terms are transformed into αβ-frame components in (9) using the simple transform of balanced systems, known as the Clarke transformation.

$$\begin{bmatrix} F_\alpha(t) \\ F_\alpha(t) \end{bmatrix} = \begin{bmatrix} 1 & -0.5 & -0.5 \\ 0 & 0.866 & -0.866 \end{bmatrix} \begin{bmatrix} F_a(t) \\ F_b(t) \\ F_c(t) \end{bmatrix} \quad (9)$$

The magnitude and sinusoidal terms of α and β components are described in (10) and (11).

$$F(t) = \sqrt{F_\alpha^2 + F_\beta^2} \quad (10)$$

$$F_\alpha(t) = F(t)\ \text{cosine}[\theta(t)]$$
$$F_\beta(t) = F(t)\ \sin[\theta(t)] \quad (11)$$

The variables, V_{alpha} and V_{beta}, shown in Figure.5 are obtained by applying this transform to the three phase o/p voltage, which is then used to calculate the output voltage's amplitude (V_o). By applying the same transformation, the current component variables I_{alpha} and I_{beta} are obtained and shown in Figure.6. These current variables, when combined with V_{alpha} and V_{beta}, constitute the signals of active and reactive power.

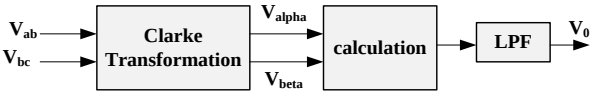

Fig. 5. αβ scheme for voltage control

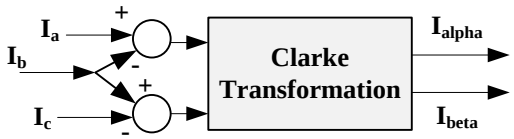

Fig. 6. αβ scheme for current control

$$p = \frac{3}{2}(i_\alpha v_\alpha + i_\beta v_\beta)$$
$$q = \frac{3}{2}(-i_\beta v_\alpha + i_\alpha v_\beta) \quad (12)$$

LPF (low pass filter) is included in the determination of o/p voltage and power components for sluggish dynamic response, harmonic and noise suppression as shown in Figure 5 and Figure 7 respectively. Their s-domain transfer functions are shown in (13), (14) and (15).

$$V_0(s) = v_0(s)\frac{\omega}{s+\omega} \quad (13)$$

$$P(s) = p(s)\frac{\omega}{s+\omega} \quad (14)$$

$$Q(s) = q(s)\frac{\omega}{s+\omega} \quad (15)$$

The MATLAB approach converts all transfer functions to a discrete-time based system model at a specified sampling rate.

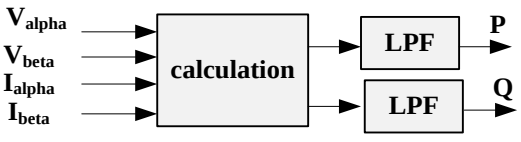

Fig. 7. Calculation of reactive and active power.

3.1 Reference voltage generation

The reference voltage generation scheme is given in Figure.8.

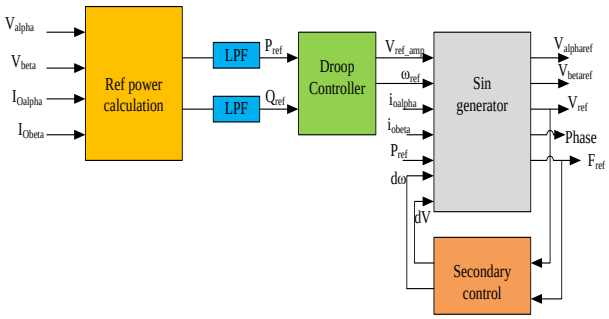

Fig. 8. Reference voltage generation scheme.

$$V_{ref} = \sqrt{V_{betaref}^2 + V_{alpharef}^2} \quad (16)$$

$$F_{ref} = \frac{\omega_{ref}}{2\pi} \quad (17)$$

The expressions described in (7) and (8) are used to obtain the design parameters with regard to the virtual impedance. l_v and R_v are designed based on dominance of impedance angle. The derivative term is decided by the cross-coupled term in (18) as angle β is 90 deg to angle α [3].

Impedance angle = $\tan^{-1}(\frac{X_v+X_g}{R_v+R_g})$ where g suffix is used for grid side.

$$Z_v i_{o\alpha} = R_v i_{o\alpha} + l_v \omega_{nom} i_{o\beta}$$
$$Z_v i_{o\beta} = R_v i_{o\beta} - l_v \omega_{nom} i_{o\alpha} \quad (18)$$

The secondary control subsystem block, shown in Figure.8, compares nominal voltage and frequency values with measured ones. This control action reduces frequency and voltage variances, restoring them to rated values. The observed error is treated by a PI controller at a specific sample rate. The PI compensators are used in each loop (V_{ref} and F_{ref}) to remove errors when comparing nominal and measured voltage and frequency values. The transfer functions of compensators are presented in (19) and (20).

$$PI_V(s) = K_{pV} + \frac{K_{iV}}{s} \quad (19)$$

$$PI_f(s) = K_{pf} + \frac{K_{if}}{s} \quad (20)$$

Subsystem Control 2, shown in Figure 9, adds variables based on network voltage readings. These variables are utilized in the functionality of PLL, which synchronises the phase between inverters 2 and 1. The function of sinusoidal generator of inverter 2 incorporates PLL synchronisation with the addition of a variable “Sig” to the secondary layer control [3]. Figure.9 shows the subsystem of the voltage reference generator.

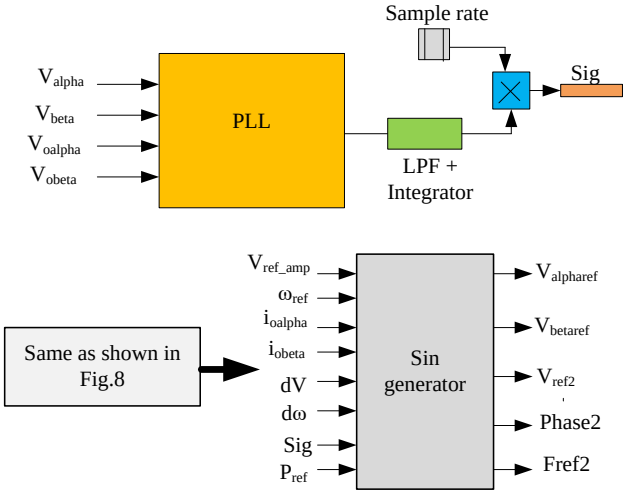

Fig. 9. Subsystem control 2 of secondary control.

The "Sig" component generated by the phase locked loop has its signal altered by a low pass filter to reduce harmonic content and offer a small dynamics for newly linked inverter, paired with an integrator controller to minimise the phase affecting both voltage values[11].

The combined T/f of an integrator and LPF is described in (21).

$$\text{Integrator + LPF} = \frac{\omega_{cPLL} K_{iPLL}}{s^2 + s\omega_{cPLL}} \quad (21)$$

The adjusted sample rate for the phase locked loop subsystem allows the synchronisation function with the V_{ref} to begin before the 2nd inverter is activated. When the 2nd inverter is synchronised with the n/w voltage and activated, it can energise the microgrid system and then participate with the power sharing functionality. The sinusoidal Generator subsystem sends reference voltage values to the current and voltage control loop subsystems. These subsystems generate M_{alpha} and M_{beta} that control half-bridge IGBT switches.

Voltage control loop subsystem consists of a PRC (proportional + resonant compensator) used to remove error that may arise when comparing V_{alpha} and $V_{alpharef}$. The output signal of PRC block is combined with the network line currents in a frame - a process known as feedforward to create $I_{alpharef}$ as depicted in Figure.10.

$$P(s) = K_{pv} \quad (22)$$

$$RC(s) = \frac{2 K_{iv} \xi \omega_{nom}\, s}{s^2 + 2\xi\omega_{nom}\, s + \omega_{nom}^2} \quad (23)$$

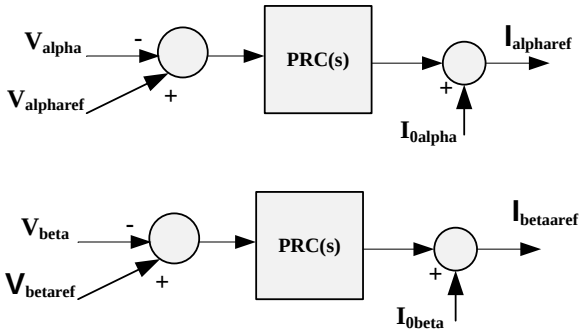

Fig. 10. Voltage control loop scheme.

An error control signal is produced by processing and eliminating the error caused by the comparison of the output current and reference current in the inner current loop control subsystem using a single PR compensator. Figure.11 illustrates the PRC system with proportional and resonant controller transfer function given in (24) and (25) [24-27].

$$P(s) = K_{pi} \quad (24)$$

$$RC(s) = \frac{2 K_{ii} \xi \omega_{nom}\, s}{s^2 + 2\xi\omega_{nom}\, s + \omega_{nom}^2} \quad (25)$$

M_{alpha} and M_{beta} are known as modulating signals, produced through the current loop control system, are transformed into pulses for each of the half-bridge switches via space vector modulation (SVM), as shown in Figure.11.

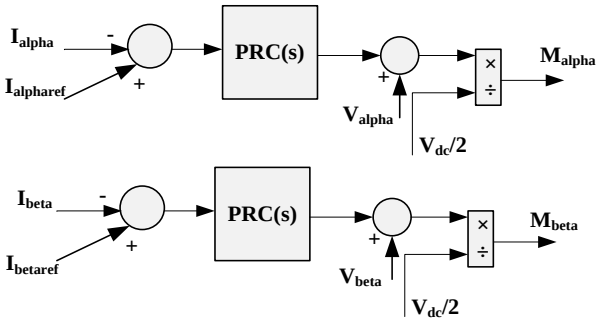

Fig. 11. Current control loop scheme.

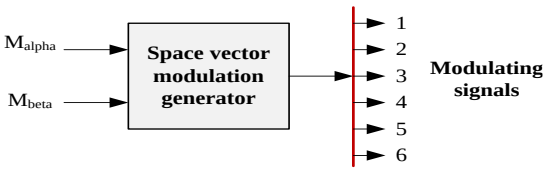

Fig. 12. SVM Scheme.

The overall scheme including reference generation, voltage and current control loop is shown in Figure.13.

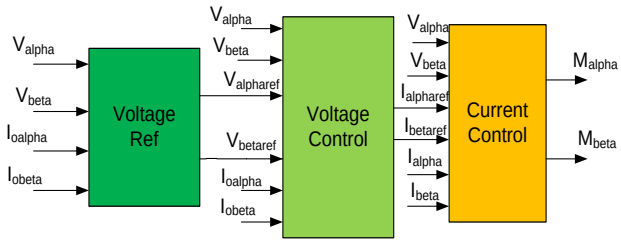

Fig. 13. Scheme of voltage and current loop control.

4. RESULT AND DISCUSSION

Scenario consists of two inverters acting as voltage sources and one common load. Besides primary droop based control, a centralized secondary control is also implemented to restore the deviations in frequency and voltage that result from primary control. Figure.14 (i-iii) illustrate active (P) and reactive power (Q) sharing, restoration of voltage and frequency.

Additional inverter in scenario will share the load after specified interval of time and it is shown in Figure.14(i). Both inverters share equal active power (P) but reactive power (Q) sharing is unequal for obvious reason as voltage works as a local variable for each inverter node. In this secondary control strategy, 1st inverter acts as the master control, while 2nd inverter serves as a slave.

Figure 14 (ii) and (iii) show steady state frequency response (equal to nominal frequency) and voltage response (equal to nominal voltage of both inverters upon action of secondary control). The current (I_{alpha}, $I_{alpharef}$) and voltage (V_{alpha}, $V_{alpharef}$) tracking in both inverters are demonstrated in Figure. 14 (IV) –(VII).

The necessary MG and control parameters are given in APPENDIX A.

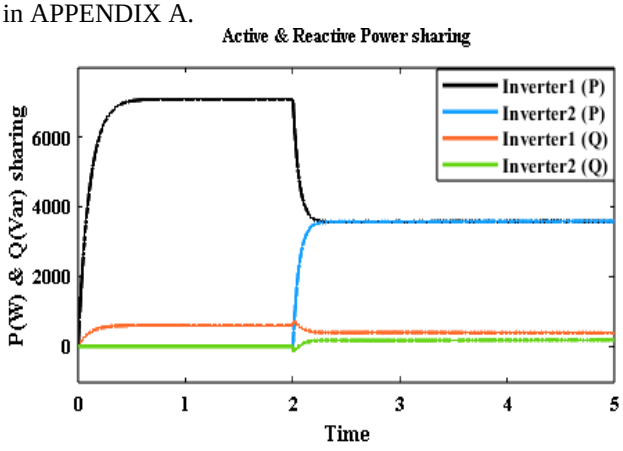

(i)

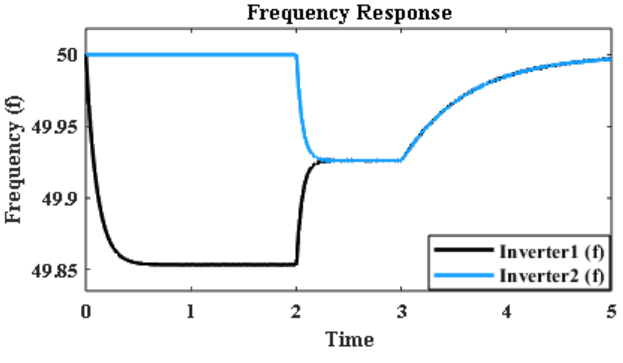

(ii)

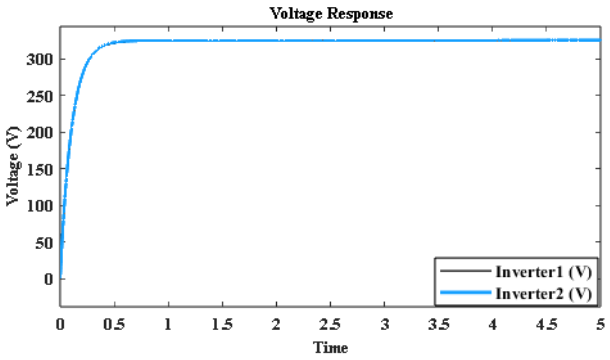

(iii)

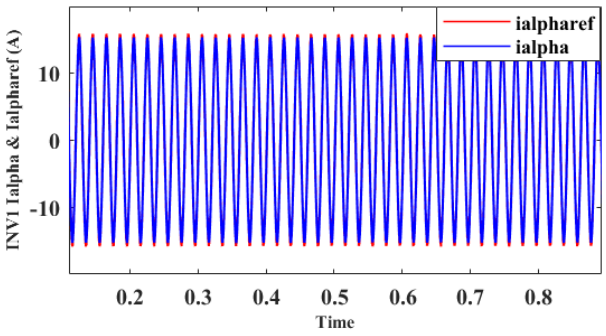

(IV)

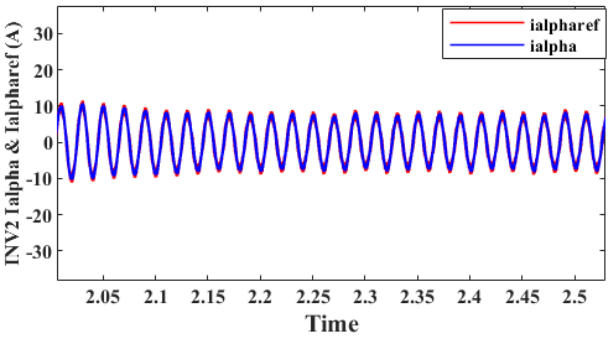

(V)

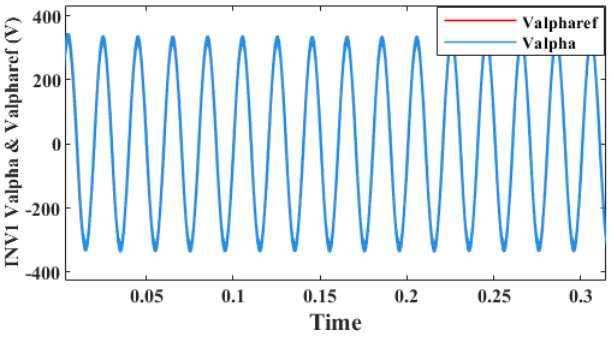

(VI)

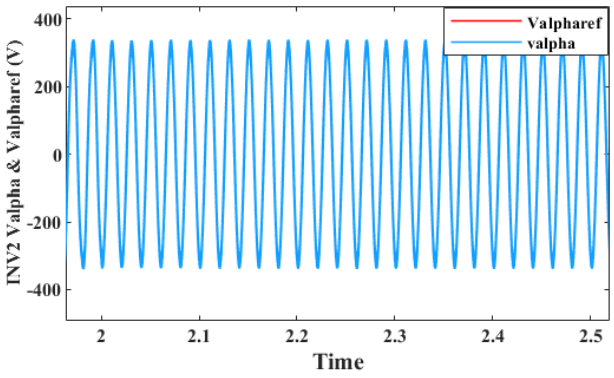

(VII)

Fig.14 (i) Active & Reactive power sharing vs time (ii) Frequency, nominal frequency vs time (iii) Voltage response vs time. (IV),(V) Ialpha & Ialpharef of INV1, INV2. (VI),(VII) Valpha & Valpharef of INV1, INV2

5. CONCLUSION AND FUTURE WORK

The paper spotlights the role of secondary layer in the hierarchy of microgrid control. Two network forming inverters are considered with a local load for illustration. Secondary control is activated after a specified time to restore frequency as well as voltage to their nominal values as a corrective measure. Control activation also ensures sharing of power between inverters as seen in the result section. The mechanism and implementation of control is described through associated models. A discretized SVM technique is utilized to convert modulating signals into pulses to drive the power electronics based inverters.

The error in reactive power mismatch between inverters upon activation of second inverter is likely to be addressed in the future work.

NOMENCLATURE

PCC: point of common coupling
n/w: network
o/p: output
SVM: space vector modulation
MG: microgrid
T/f: transfer function
PLL: phase locked loop
DG: distributed generator
LPF: low pass filter
PRC: proportional resonant compensator
VI: virtual impedance
MATLAB: matrix laboratory
INV: inverter
CDC: conventional droop control
BW: bandwidth

REFERENCES

[1] Bhambri, S., Kumawat, M., Shrivastava, V., Agarwal, U., Jain N.K., 2023. The Energy Mix: An Emerging Trend in Distribution System. In: Singh, S.N., Jain, N., Agarwal, U., Kumawat, M. (eds) *Optimal Planning and Operation of Distributed Energy Resources. Energy Systems in Electrical Engineering*. Springer, Singapore, pp. 11-37.

[2] Cheng Z., Duan J. and Chow M. Y., 2018. To Centralize or to Distribute: That Is the Question: A Comparison of Advanced Microgrid Management Systems, *IEEE Industrial Electronics Magazine*,12(1): 6-24.

[3] de Souza Z .C .A. and Castilla M., 2019. *Microgrids design and implementation*, 1st edn. Springer, Cham.

[4] Martí P., Velasco M., Martín E. X., de Vicuña L. G., Miret J. and Castilla M., 2018. Performance Evaluation of Secondary Control Policies With Respect to Digital Communications Properties in Inverter-Based Islanded Microgrids, *IEEE Transactions on Smart Grid*, 9 (3): 2192-2202.

[5] Liserre M., Teodorescu R. and Blaabjerg F., 2006. Stability of photovoltaic and wind turbine grid-connected inverters for a large set of grid impedance values, *IEEE Transactions on Power Electronics*, 21(1): 263-272.

[6] Miret J., García de Vicuña L J., Guzmán R., Camacho A. and Ghahderijani M. M., 2017 A flexible experimental laboratory for distributed generation networks based on power inverters. *Energies* 10(10):1589.

[7] Guerrero J.M., Chandorkar M., Lee T.L. and Loh P.C., 2013. Advanced Control Architectures for Intelligent Microgrids—Part I: Decentralized and Hierarchical Control. *IEEE Transactions on Industrial Electronics*. 60(4): 1254-1262.

[8] Yazdani A. and Iravani R., 2010. Voltage-sourced converters in power systems, vol 34. *Wiley Online Library*, New Jersey.

[9] Fagarasan I., Stamatescu I., Arghira N., Hossu D., Hossu A. and Iliescu S S., 2017. Control Techniques and Strategies for Microgrids: Towards an Intelligent Control. *21st International Conference on Control Systems and Computer Science (CSCS)*. Bucharest, Romania, 7 July.IEEE.

[10] Guerrero J. M, Vasquez J.C., Matas J., de Vicuña L.G. and Castilla M., 2011. Hierarchical Control of Droop-Controlled AC and DC Microgrids—A General Approach Toward Standardization. *IEEE Transactions on Industrial Electronics*. 58(1): 158-172.

[11] Rocabert J., Azevedo G M S, Luna A, Guerrero J. M., Candela J. I. and Rodríguez P., 2011. Intelligent Connection Agent for Three-Phase Grid- Connected Microgrids. *IEEE Transactions on Power Electronics*. 26(10): 2993-3005.

[12] Saeed M. H, Fangzong W., Kalwar B. A, and Iqbal S., 2021 Review on Microgrids Challenges & Perspectives. *IEEE Access*. 9:166502-166517.

[13] Tayab U. B., Roslan M.A.B., Hwai L. J. and Kashif M., 2017 A review of droop control techniques for rnicrogrid. *Renew. Sust. Energ. Rev.* 76:717-727.

[14] Bhambri S., Shrivastava V. and Kumawat M., 2023. Single Solution for Control and Synchronization of Inverters in Microgrids. *9th IEEE India International Conference on Power Electronics (IICPE)*,Sonipat, India, 28-30 November.IEEE.

[15] Zhong Q.C., 2013 Robust Droop Controller for Accurate Proportional Load Sharing Among Inverters Operated in Parallel .*IEEE Trans. Ind. Electron*. 60(4): 1281–1290.

[16] Zhong Q. C. and Zeng Y., 2013 Control of Inverters Via a Virtual Capacitor to Achieve Capacitive Output Impedance . *IEEE Transactions on Power Electronics*. 29(10):5568-5578.

[17] Zhong Chang Qing and Zeng Yu, 2016 Universal Droop Control of Inverters With Different Types of Output Impedance. *IEEE Access*, vol. 4, pp. 702-712.

[18] Lazzarin T. B., Bauer G.A.T. and Barbi I., 2013 A Control Strategy for Parallel Operation of Single-Phase Voltage Source Inverters: Analysis, Design and Experimental Results . *IEEE Transactions On Industrial Electronics*. 60(6):2194-2204.

[19] Yao Zhilei. and Xiao Lan., 2013 Control of Single-Phase Grid Connected Inverters With Nonlinear Loads . *IEEE Transactions on Industrial Electronics*, pp. 1384-1389.

[20] Micallef A Apap., M Spiteri-Staines C and Guerrero J. M., 2016. Performance Comparison for Virtual Impedance Techniques Used in Droop Controlled Islanded Microgrids. *IEEE International Symposium on Power Electronics, Electrical Drives, Automation and Motion (SPEEDAM).* pp. 695 – 700.

[21] Micallef A. Apap., M Spiteri-Staines C and Guerrero J M., 2016. Mitigation of Harmonics in Grid-Connected and Islanded Microgrids Via Virtual Admittances and Impedances *IEEE Trans. Smart Grid*, PP(99): 1–11.

[22] S. Bhambri., V. Shrivastava., M. Kumawat and S. Agrawal., 2024. Modelling and Control of Microgrids in an Offgrid Operating Scenario: A Case Study. *IEEE Region 10 Symposium (TENSYMP)*, New Delhi, India, 27-28 September.IEEE.

[23] S. Bhambri., V. Shrivastava and M. Kumawat., 2024. Performance Improvement in Droop Controlled Islanded Microgrids via Selective Harmonic Control. *International Conference on Power Electronics, Intelligent Control and Energy Systems (ICPEICES)*. New Delhi, India, 26-28 April. IEEE.

[24] Pournazarian B., Seyedalipour S. S., Lehtonen M., Taheri S. and Pouresmaeil E., 2020. Virtual Impedances Optimization to Enhance Microgrid Small-Signal Stability and Reactive Power Sharing. *IEEE Access*, 8: 139691-139705.

[25] Pournazarian B., Sangrody R., Lehtonen M., Gharehpetian B. G. and Pouresmaeil E., 2022. Simultaneous Optimization of Virtual Synchronous Generators Parameters and Virtual Impedances in Islanded Microgrids. *IEEE Transactions on Smart Grid*.13(6): 4202-4217.

[26] Yu K., Ai Q., Wang S., Ni J. and Lv T., 2016. Analysis and Optimization of Droop Controller for Microgrid System Based on Small-Signal Dynamic Model. *IEEE Transactions on Smart Grid*. 7(2): 695-705.

[27] Rasheduzzaman Md., Mueller J.A. and Kimball J. W., 2014. An Accurate Small-Signal Model of Inverter- Dominated Islanded Microgrids Using dq Reference Frame. *IEEE Journal of Emerging and Selected Topics in Power Electronics*. 2(4): 1070-1080.

APPENDIX A

Control parameters of microgrid are given in Table.2.

Table. 2. MG and its control parameters.

Parameter	Denotion	Value	Unit
DC voltage	V_{DC}	800	V
Frequency- active power droop coefficient	m_d	125	microrad/Ws
Frequency-active power derivative droop coefficient	m_{dp}	9.5	microrad/W
Voltage-reactive power droop coefficient	n_d	0.95	milliV/Var
Virtual inductance	L_v	0.9	milliH
Virtual resistance	R_v	0	Ω
Proportional gain value of PRC voltage controller	K_{pv}	0.1	A/V
Integral gain value of PRC voltage controller	K_{iv}	0.1	A/Vs
Damping coefficient of PRC voltage controller	ξ	0.01	
Proportional gain value of PRC current controller	K_{pi}	12	A/V
Integral gain value of PRC current controller	K_{ii}	200	A/Vs
Damping coefficient of PRC current controller	ξ	0.1	
Output resistance of inverter1	R_{o1}	0.5	Ω
Output inductance of inverter1	L_{o1}	5	milliH
Filter capacitance	C_{f1}	10	microF
Damping resistance	R_{f1}	18.5	Ω
Line resistance	R_{L1}	0.065	Ω
Line inductance	L_{L1}	1	milliH
Cutoff frequency of LPF	ω_c	11	rad/s
Proportional gain of secondary control (voltage correction)	K_p	0.1	
Integral gain of secondary control (voltage correction)	K_i	0.2	
Proportional gain of secondary control (frequency correction)	K_p	0.0001	

Integral gain of secondary control (frequency correction)	K_i	9.5

The parameter values of second inverter (output resistance, inductance, filter capacitance,damping resistance, line resistance and inductance) are 1.15 times the corresponding values of the first inverter.